



## Research Paper

# MicroR-146 blocks the activation of M1 macrophage by targeting signal transducer and activator of transcription 1 in hepatic schistosomiasis



Xing He<sup>a,1</sup>, Rui Tang<sup>a,b,1</sup>, Yue Sun<sup>a,b</sup>, Yan-Ge Wang<sup>a</sup>, Kui-Yang Zhen<sup>a</sup>, Dong-Mei Zhang<sup>a,\*</sup>, Wei-Qing Pan<sup>a,\*</sup>

<sup>a</sup> Department of Tropical Infectious Diseases, Second Military Medical University, Shanghai 200433, China

<sup>b</sup> Department of Pathogen Biology, Xuzhou Medical University, Xuzhou 221000, China

## ARTICLE INFO

## Article history:

Received 15 August 2016

Received in revised form 15 October 2016

Accepted 18 October 2016

Available online 19 October 2016

## Keywords:

miR-146

macrophage differentiation

hepatic schistosomiasis

STAT pathway

## ABSTRACT

Schistosomiasis is a chronic disease caused by the parasite of the *Schistosoma* genus and is characterized by egg-induced hepatic granulomas and fibrosis. Macrophages play a central role in schistosomiasis with several studies highlighting their differentiation into M2 cells involved in the survival of infected mice through limitation of immunopathology. However, little is known regarding the mechanisms of regulating macrophage differentiation. Here, we showed that the early stage of infection by *Schistosoma japonicum* induced expression of type 1 T-helper-cell (Th1) cytokine, interferon- $\gamma$  (IFN- $\gamma$ ), leading to increase in M1 cells. However, the presence of liver-trapped eggs induced the expression of Th2 cytokines including interleukin-4 (IL-4), IL-10, and IL-13 that upregulated the transcription of *miR-146b* by activating signal transducer and activator of transcription 3/6 (STAT3/6) that bind to the promoter of the *pre-miR-146b* gene. We found that the miR-146a/b was significantly upregulated in macrophages during the progression of hepatic schistosomiasis. The elevated miR-146a/b inhibited the IFN- $\gamma$ -induced differentiation of macrophages to M1 cells through targeting STAT1. Our data indicate the protective roles of miR-146a/b in hepatic schistosomiasis through regulating the differentiation of macrophages into M2 cells.

© 2016 The Authors. Published by Elsevier B.V. This is an open access article under the CC BY-NC-ND license (<http://creativecommons.org/licenses/by-nc-nd/4.0/>).

## 1. Introduction

Schistosomiasis is a neglected tropical and sub-tropical parasitic disease, caused by blood-dwelling fluke worms of the genus *Schistosoma*, affecting >230 million people worldwide (Colley et al., 2014). The primary pathology of schistosomiasis is egg-induced granuloma and fibrosis, which is a result of the host immune response to the eggs. In the early phase of infection, a type 1 T-helper-cell (Th1) response is induced by the migration of the schistosomula and adult worms and is characterized by the elevation of interferon- $\gamma$  (IFN- $\gamma$ ) levels. Host immune response is later polarized into a Th2 response, initiated by the release of eggs occurring 4–6 weeks post-infection, featuring an increase in the levels of interleukin-4 (IL-4), IL-13, etc. (Pearce and MacDonald, 2002; Burke et al., 2009). These Th1 and Th2-related cytokines play a decisive role in the pathogenesis of schistosomiasis.

Macrophages play a vital role in the liver pathology caused by *Schistosoma* (Barron and Wynn, 2011). They regulate the initiation,

maintenance, and resolution of this chronic inflammatory disease and their function depends on their activation status. Macrophages can be classically activated (M1 macrophages) or alternatively activated (M2 macrophages) depending on the local immune environment (Kreider et al., 2007; Noël et al., 2004; Sica and Mantovani, 2012). M1 macrophages are induced by Th1 cytokines or microbial molecules such as lipopolysaccharide (LPS), while M2 macrophages are stimulated by Th2 cytokines. M1 macrophages primarily produce pro-inflammatory cytokines such as tumour necrosis factor  $\alpha$  (TNF- $\alpha$ ), IL-1 $\beta$ , IL-12, and IL-23. M2 macrophages are involved in Th2-biased response producing cytokines such as transforming growth factor  $\beta$  (TGF- $\beta$ ) and IL-10 leading to parasite clearance and host protection.

MicroRNAs (miRNAs) are a class of endogenous, small noncoding RNA molecules, which control the translation and transcription of many genes (Bartel, 2004, 2009; Ma et al., 2011). Numerous studies have demonstrated that miRNAs play a crucial role in many human diseases including schistosomiasis (He et al., 2013, 2015; Cai et al., 2013, 2016; Han et al., 2013). Our previous study using miRNA microarrays demonstrated that a series of miRNAs were deregulated in the progression of hepatic schistosomiasis in a mouse model. Importantly, miR-21, one of the upregulated miRNAs, was involved in the regulation of activation of hepatic stellate cells (HSCs) and downregulation of miR-21 prevented lethal infection by repressing both TGF- $\beta$ 1 and IL-13 pathways (He et al., 2015).

\* Corresponding authors at: Department of Tropical Infectious Diseases, Second Military Medical University, 8 Panshan Road, Yangpu District, Shanghai 200433, China.

E-mail addresses: [dmzhangcn@163.com](mailto:dmzhangcn@163.com) (D.-M. Zhang), [wqpan0912@aliyun.com](mailto:wqpan0912@aliyun.com) (W.-Q. Pan).

<sup>1</sup> These authors contribute equally to this study.

In this study, we used a murine model of *Schistosoma japonicum* (*S. japonicum*) to investigate the roles of miR-146a/b, two upregulated miRNAs identified in our previous study (He et al., 2015), in the progression of hepatic schistosomiasis. We found miR-146 was primarily expressed in hepatic macrophages, and inhibited the differentiation of macrophages to M1 cells by targeting signal transducer and activator of transcription 1 (STAT1), a crucial molecule in IFN- $\gamma$  signalling. In addition, a series of Th2 cytokines, including IL-4, IL-10, and IL-13, induced the expression of miR-146b by activating STAT3/6 in macrophages, and thus prevented the differentiation of macrophages into M1 cells.

## 2. Methods

### 2.1. Ethics statement

All animal experiments were undertaken in strict accordance with the Guide for the Care and Use of Laboratory Animals of the National Institutes of Health, and were approved by the Animal Ethics Committee of Second Military Medical University (laboratory animal usage number FYXK (Shanghai) 2014–0003). To minimize pain and discomfort, all animal surgeries were performed under sodium pentobarbital anaesthesia. All mice used in this study were purchased from the Experimental Animal Center of the Second Military Medical University, and were housed in specific pathogen-free conditions and fed autoclaved food and water as needed.

### 2.2. Schistosome infection and sample preparation

To establish the animal model of schistosomiasis, six-week-old BABL/c male mice were exposed percutaneously to 16 *S. japonicum* cercariae shed from lab-infected snails (*Oncomelania hupensis*), obtained from the Institute of Parasitic Disease, Shanghai.

For collection of liver samples, 24 mice were infected and six mice each were sacrificed on days 21, 32, 42 and 52 post-infection. In addition, six uninfected mice were used as control samples and were sacrificed on day 0. To collect blood from the portal vein, the abdominal cavity of mouse was opened after anesthetization, then portal vein was penetrated with sterile single-use syringe for insulin to drain blood. After collecting blood, portal vein was dissected at the root, then the thoracic cavity of mouse was opened and the circulatory system was perfused via the aorta with 20 mL of sterile PBS, and worms were collected and counted in a sterile petri dish containing medium as described previously (Shainheit et al., 2008). Subsequently, liver samples were removed and snap frozen in liquid nitrogen.

After sample collection, mice were killed by cervical dislocation.

For collection of primary liver cell samples, another 24 mice were infected and six mice each were sacrificed on days 21, 32, 42 and 52 post-infection. In addition, six uninfected mice were used as control samples and were sacrificed on day 0. After *in situ* digestion with collagenase, livers were dissected and the mice were killed by cervical dislocation.

### 2.3. Isolation of mouse hepatocytes, HSCs and hepatic macrophages

The procedure was followed as described previously (He et al., 2014). The hepatic macrophages were first isolated by density-gradient centrifugation and then purified using positive selection with magnetic CD11b antibody beads (MACS, Miltenyi, Auburn, CA). In this study, hepatic macrophages were defined as CD11b positive cells, and the purity was determined to be >90% using FACS-Calibur analysis after labelling purified cells with anti-CD11b-FITC antibody (Miltenyi) (Fig. S1).

### 2.4. Liver pathology

Liver specimens were fixed in 5% (v/v) paraformaldehyde, and the size of hepatic granuloma and the extent of fibrosis were observed by H&E staining and Masson's trichrome staining of liver sections.

### 2.5. Egg counting

After liver tissue was digested overnight with 4% potassium hydroxide, the total number of schistosome eggs in the liver tissue was counted, and the liver egg burdens were defined as  $10^4$  eggs per gram of liver tissue.

### 2.6. Cell culture and stimulation

BMDMs were isolated from 6 to 8-week-old BABL/c male mice as described (Davis, 2013). Primary cells were maintained on bacterial grade plates for 1 week in DMEM (Hyclone), supplemented with 10% fetal bovine serum (Hyclone), 2 mM L-glutamine, 100 units/mL penicillin G, 100 mg/mL streptomycin (Invitrogen) and 5 ng/mL M-CSF (ProSpec). Adherent cells were then replated on plastic tissue culture plates in fresh media and used 24 h after replating. The immortalized rat Kupffer cell line (purchased from Applied Biological Materials Inc.) was maintained in the same media as BMDMs but without M-CSF.

For stimulation, BMDMs or the Kupffer cell line were exposed to recombinant IFN- $\gamma$ , IL-10, IL-4 or IL-13 (ProSpec) after starvation overnight in 0.5% fetal bovine serum (Hyclone), and harvested at the appropriate time points.

For transfection, 40 nM miRNA mimics, inhibitors or negative control (GenePharma, China) was transfected using the Lipofectamine 2000 Transfection Reagent (Life technologies) according to the manufacturer's instructions.

### 2.7. RNA extraction and real-time PCR

Total RNA was extracted using Trizol reagent (Invitrogen) according to the manufacturer's protocol. Real-time PCR was performed as described previously (Schmittgen and Livak, 2008). The expression of miR-146a, miR-146b, IFN- $\gamma$ , TNF- $\alpha$ , IL-4, IL-10, IL-13, TGF- $\beta$ 1, iNOS and Arg-1 was determined using the SYBR Green Master Mix kit (Takara). GAPDH or U6 snRNAs was used as the internal control for mRNA or miRNA quantification, and the fold change was calculated using the  $2^{-\Delta\Delta Ct}$  method. Supplementary Table S1 shows the primer sequences used in this study.

### 2.8. Western blotting

Cell protein was extracted on ice using RIPA lysis buffer (Beyotime) in the presence of a freshly added cocktail of protease inhibitors (Thermo), and then quantified by the BCA method (Pierce). A total of 30  $\mu$ g total protein per lane was loaded onto 12% SDS-polyacrylamide gels, electrophoresed, and then transferred to 0.2- $\mu$ m nitrocellulose membranes (Pierce) for 1 h at 350 mA using a wet western blotting system. After blocking with 5% non-fat milk in PBS, the membrane was incubated with rabbit anti-STAT1 antibody (Epitomics, Cat. 2251–1) or rabbit anti-phospho-STAT1 (CST, Cat. 7649) overnight at 4 °C. IRDye 800CW goat anti-rabbit IgG (LI-COR, Cat. 926–32,211) was used as secondary antibody to display the signal, and rabbit anti-GAPDH (Epitomics, Cat. 2251–1) antibody was used as an internal standard.

### 2.9. ChIP Assay

ChIP experiments were performed as described elsewhere (Lee et al., 2006). Sheared chromatin from  $5 \times 10^6$  BMDMs was immunoprecipitated overnight at 4 °C using monoclonal rabbit anti-STAT3 (CST, Cat.5397) or monoclonal rabbit anti-STAT6 (CST, Cat.4904). One percent of the initial chromatin, not immunoprecipitated, was used as the input. Quantitative real-time PCR (qPCR) was performed in triplicate by using promoter-specific primers (Table S1). Signals from ChIP samples were normalized to signals from corresponding input samples, calculated according to the formula  $100 \times 2^{(\text{input Ct} - \text{ChIP Ct})}$ . Results are expressed in fold-enrichment relative to control samples.

### 2.10. Detection of LPS level in serum

LPS levels in serum from portal vein were detected using a colourmetric assay according to manufacturer's instructions (Chinese Horseshoe Crab Reagent Manufactory Co., Ltd., China). The minimum detectable concentration of the kit was 0.01 EU/mL.

### 2.11. Luciferase Reporter Assay

The miR-146b promoter were amplified from genomic DNA from BMDMs and cloned in the pGL3-Basic vector (Promega). The structures of all constructs were confirmed by DNA sequence analysis. For promoter luciferase reporter assays, BMDMs were plated at  $10^5$  cells per well in 24-well dishes, and were transiently transfected with the indicated constructs and pRL-TK-Renilla for 24 h using the Lipofectamine 2000 Transfection Reagent (Life technologies) according to the manufacturer's instructions, and then the cells were incubated with IL-4, IL-10 or IL-13. After 12 h, the cells were harvested for the luciferase activity assay.

### 2.12. Statistical analyses

All results are reported as means  $\pm$  standard deviations. Statistical evaluation between groups was performed by two-tailed Student's *t*-test or one-way ANOVA and is presented in the Figures. *P*-values <0.05 were considered statistically significant.

## 3. Results

### 3.1. Expression of miR-146 in the progression of hepatic schistosomiasis

Liver samples from mice at various time points after *S. japonicum* infection were collected to analyse liver pathology and miR-146 expression in the progression of hepatic schistosomiasis. The results of hematoxylin and eosin (H&E) staining of liver sections revealed mild inflammation along with the presence of eggs in the liver tissue starting from day 32 post-infection. By day 42 post-infection, eggs were encompassed by a large population of inflammatory cells, resulting in the formation of a mature granuloma with mild extracellular matrix (ECM) deposition (Fig. S2a). The number of worm pairs in the mesenteric veins of mice showed no change during the parasite infection (Fig. S2b), but the egg burden in liver tissues dramatically increased after day 32 post-infection (Fig. S2c).

In our previous study, we have shown using miRNA microarrays that the expression of miR-146 was increased in liver tissues after *S. japonicum* infection (He et al., 2015), a similar result was confirmed by RNA-seq method (Cai et al., 2013). To validate these microarray results, we looked at the expression of miR-146 in liver tissues by real-time PCR (RT-PCR). As shown in Fig. 1a and b, the expression levels of both miR-146a and miR-146b in the liver tissues were significantly elevated by day 32 post-infection compared to that on day 0 ( $p < 0.001$ ), and peaked at day 42 post-infection followed by a decrease at day 52. It is well acknowledged that the role of miRNAs is cell-type specific, thus we isolated different types of

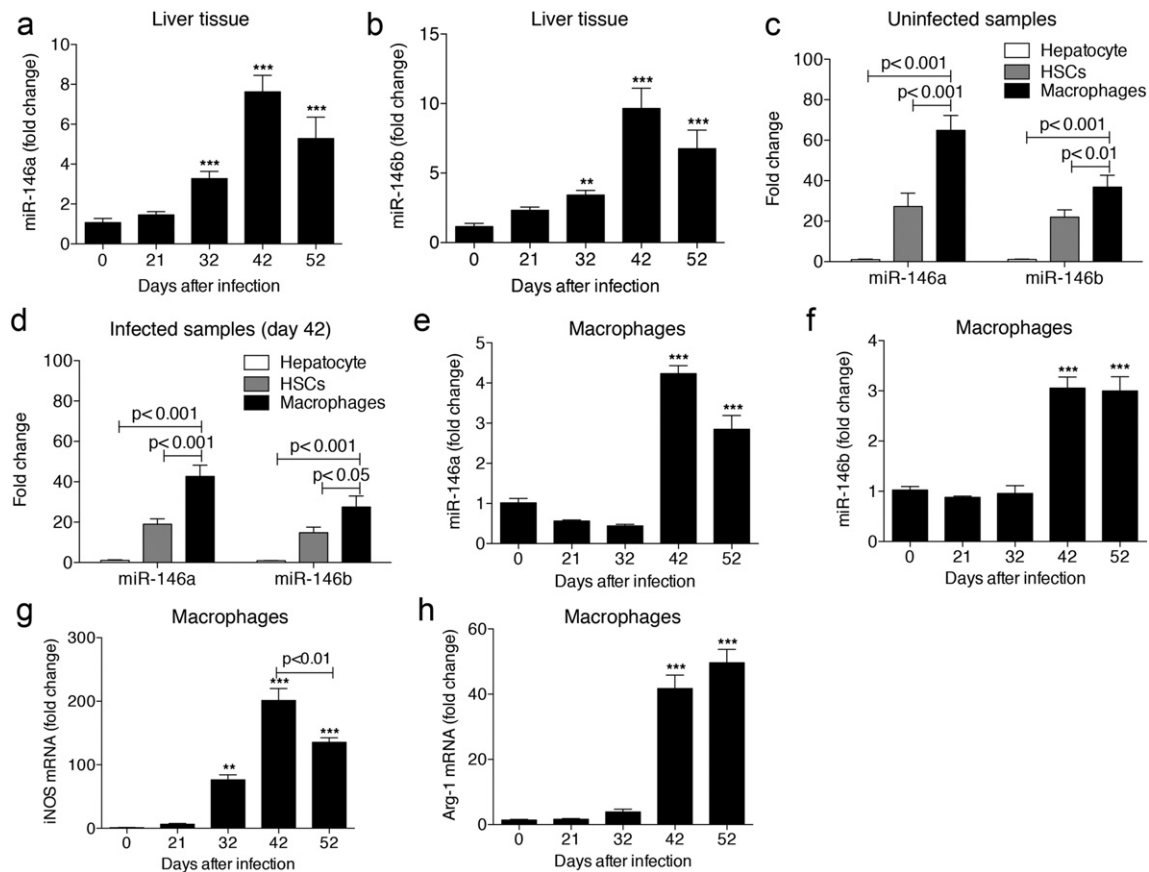


**Fig. 1.** Expression of miR-146 in liver after *S. japonicum* infection. (a, b) Change in miR-146a (a) and miR-146b (b) levels in liver cells after infection. \*\* $P < 0.01$ , \*\*\* $P < 0.001$ , compared with samples from uninfected mice (day 0). (c, d) Hepatocytes, HSCs and macrophages were isolated from uninfected (c) and infected (d) livers (day 42 after infection), and the levels of miR-146a or miR-146b in HSCs and macrophages were compared to that in hepatocytes, respectively. (e, f, g, h) Change in miR-146a (e), miR-146b (f), iNOS (g) and Arg-1 (h) levels in macrophages after infection. \*\* $P < 0.01$ , \*\*\* $P < 0.001$ , compared with samples from uninfected mice (day 0). Data are shown as means with SDs. Data in all panels are representative of three independent experiments.

liver cells from infected and uninfected livers, and detected their expression. We found that the abundance of miR-146a and miR-146b in hepatic macrophages was significantly higher than that in other cell types such as hepatocytes and HSCs in the livers of both uninfected and infected (day 42 post-infection) mice (Fig. 1c and d), suggesting that miR-146 could be involved in the regulation of the function of hepatic macrophages. It is worthy to point out that the fold change in hepatic macrophages from uninfected mice was greater than that from infected mice. This is because the level of miR-146 in uninfected hepatocytes was much lower than that in the infected hepatocytes (Fig. S3), while all the fold changes were calculated via comparison with the levels of uninfected or infected hepatocytes, respectively. In addition, we analysed the expression of miR-146 in macrophages during the progression of hepatic schistosomiasis. We found that both miR-146a and miR-146b were upregulated in macrophages by day 42 post-infection compared to that in uninfected liver. The peaks of miR-146a and miR-146b expression were similar (Fig. 1e and f).

### 3.2. miR-146 regulates the differentiation of macrophages in hepatic schistosomiasis

We analysed the alteration of the immune environment in liver and the activation status of macrophages in the progression of hepatic schistosomiasis. The expression of the Th1 cytokine, such as IFN- $\gamma$ , was significantly increased during the early stage of infection and then decreased gradually after 32 days post-infection (Fig. S4a and S4b). However, the expression of the Th2 cytokine was dramatically elevated at later time points (day 42 and 52 post-infection) (Fig. S4c–4f). However, the level of LPS in portal vein serum did not change during the observed time period (Fig. S5).

Inducible nitric oxide synthase (iNOS) is a marker of M1 macrophages while arginase 1 (Arg-1) is an M2 marker. As shown in Fig. 1g and h, iNOS expression increased by day 32 and peaked at day 42, followed by a decrease at day 52. Contrarily, Arg-1 expression was

significantly upregulated by day 42 and the highest expression level was observed on day 52. The concomitant alteration in the expression of both iNOS and miR-146 in macrophages led us to the question whether miR-146 could inhibit the differentiation of macrophages into M1 cells. In order to test this, a Kupffer cell line was transfected with miR-146a and miR-146b, respectively, and then stimulated with IFN- $\gamma$ . Our data showed a significant decrease in the expression of iNOS and TNF- $\alpha$  in Kupffer cells transfected with miR-146a and miR-146b and stimulated by IFN- $\gamma$  (Fig. 2a and b). The expression of M2 markers, Arg-1 and TGF- $\beta$ 1 remained unchanged (Fig. 2c and d). This suggests that both miR-146a and miR-146b affect the differentiation of macrophages into M1 cells. Further, we verified this phenomenon by using bone marrow derived macrophages (BMDMs), where both miR-146a and miR-146b inhibited the IFN- $\gamma$ -induced differentiation into M1 cells with a significant reduction in the expression levels of M1 markers (Fig. S6).

### 3.3. STAT1 is a target of miR-146 in macrophages

STAT1 is a pivotal molecule in IFN- $\gamma$  signal transduction, thus this molecule could play an important role in M1 activation. It is intriguing that STAT1 is a predicted target of miR-146 in the TargetScan database, which was validated in regulatory T cells (Lu et al., 2010) and also in peripheral blood mononuclear cells (Tang et al., 2009). To analyse the relationship between miR-146 and STAT1 in macrophages, we detected the expression pattern of STAT1 in hepatic macrophages with the progression of hepatic schistosomiasis. We found that STAT1 expression in hepatic macrophages was elevated at day 21 and 32, followed by a dramatic decrease at day 42 and 52 (Fig. 3a), which contrasts with the expression pattern of miR-146 in macrophages (Fig. 1e and f), implying that miR-146 could regulate STAT1 expression. Further, we transfected miR-146a/b into the Kupffer cell line and detected the expression of STAT1 by RT-PCR. As shown in Fig. 3b, miR-146 significantly inhibited the expression of STAT1 in Kupffer cell. This result was also validated

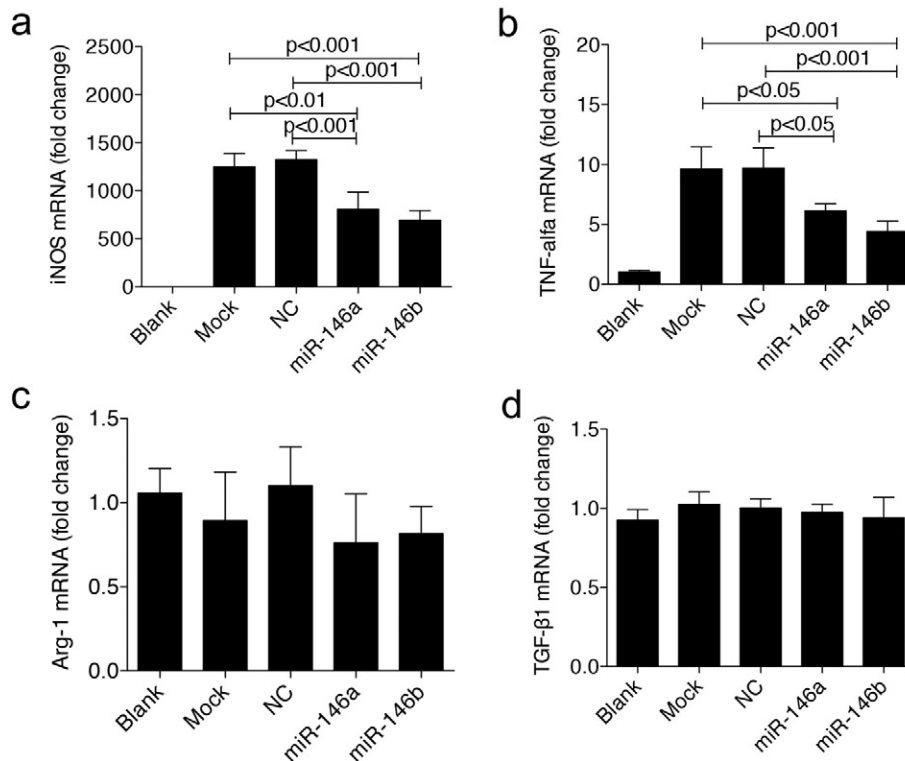


**Fig. 2.** miR-146 blocked the differentiation of macrophages to M1 cells. A Kupffer cell line was transfected with 40 nM miR-146a, miR-146b mimics, a negative control miRNA (NC), or transfection reagent only (mock) for 24 h, then stimulated with IFN- $\gamma$  for 24 h. Total RNA was collected and analysed for expression of iNOS (a), TNF- $\alpha$  (b), Arg-1 (c), or TGF- $\beta$ 1 (d) by qPCR. Data are shown as means with SDs. Data in all panels are representative of four independent experiments.

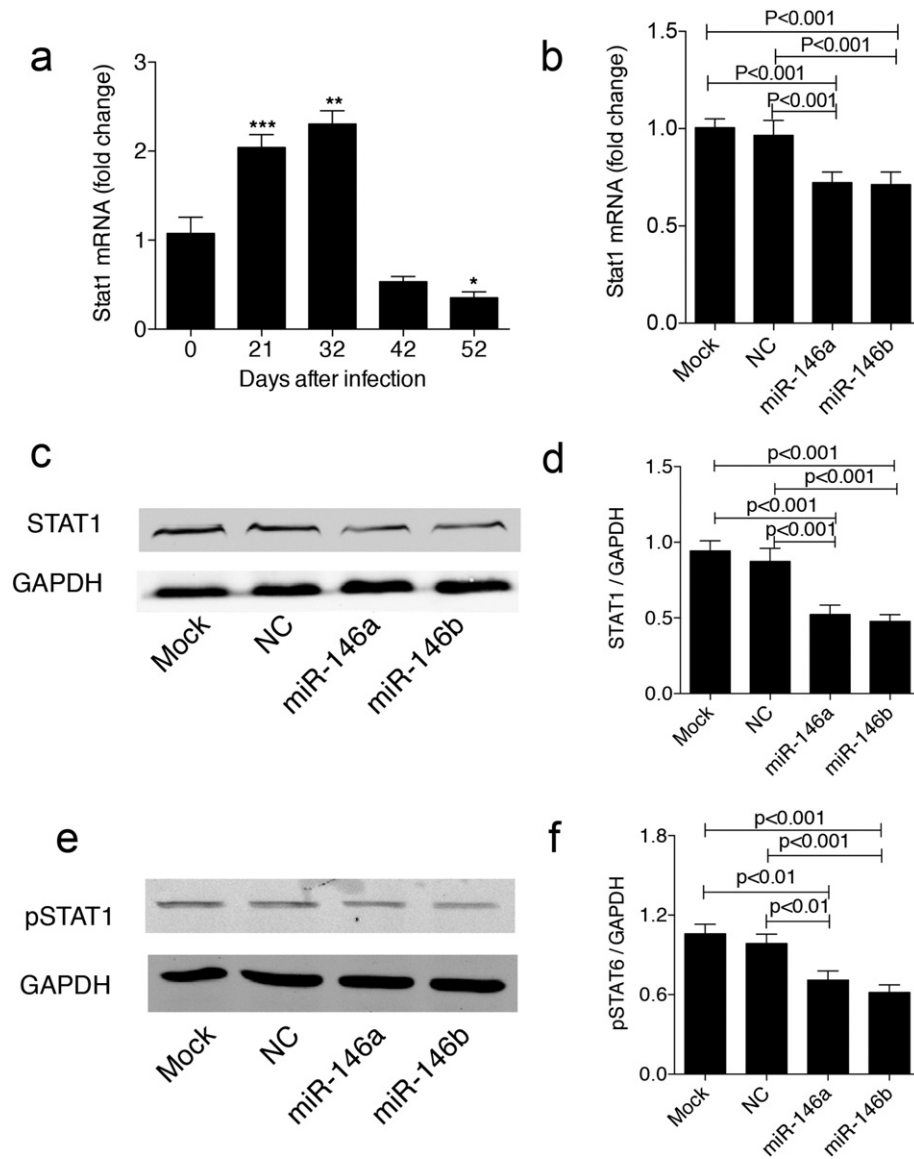


**Fig. 3.** Target validation of miR-146. (a) STAT1 expression in hepatic macrophages after *S. japonicum* infection. \* $P < 0.05$ , \*\* $P < 0.01$ , \*\*\* $P < 0.001$ , compared with samples from uninfected mice (day 0). (b, c, d) A Kupffer cell line was transfected with 40 nM miR-146a, miR-146b mimics, a negative control miRNA (NC), or transfection reagent only (mock) for 48 h, then total RNA and protein were collected and analysed for expression of STAT1 by qPCR (b) and western blot (c, d), respectively. (e, f) A Kupffer cell line was transfected with 40 nM miR-146a, miR-146b mimics, a negative control miRNA (NC), or transfection reagent only (mock) for 42 h, then stimulated with IFN- $\gamma$  for 6 h, and total protein was collected and analysed for expression of phospho-STAT1 by western blot. Data are shown as means with SDs. Data in all panels are representative of three independent experiments.

by western blotting (Fig. 3c and d). Further, we repeated the experiment using BMDMs of mice and found that miR-146a/b transfection significantly inhibited STAT1 expression in BMDMs (Fig. S7). These data demonstrated that STAT1 is a target of miR-146 in macrophages. In addition, STAT1 phosphorylation is responsible for the definitive function of STAT1, thus, we analysed the effect of miR-146a/b on STAT1 phosphorylation, and we found, as expected, when the Kupffer cells were transfected with miR-146a or b in advance, the phosphorylated STAT1 in Kupffer cells after IFN- $\gamma$  stimulation was obviously decreased (Fig. 3e and f).

#### 3.4. Th2 cytokines induced the expression of miR-146b in BMDMs

The interplay of various cytokines, including both Th1 and Th2 cytokines, has a crucial role in the pathology and progression of hepatic schistosomiasis. Thus, we speculated whether the expression of miR-146 in hepatic macrophages is modulated by the cytokines. We noticed that the expression of all the Th2 cytokines (IL-4, IL-10, IL-13 and TGF- $\beta$ 1)

in the livers were upregulated post-infection (Fig. S4c–4f), and were correlated with the expression pattern of miR-146 in the livers (Fig. 1a and b). To determine whether these cytokines regulated the expression of miR-146, we stimulated BMDMs with recombinant cytokines *in vitro*. As shown in Fig. 4a and b, IL-4, IL-10, and IL-13 significantly induced the expression of miR-146b, but not miR-146a. Next, we investigate the molecular pathway leading to the induction of miR-146b expression by the cytokines. The mouse *pre-miR-146b* gene resides in the first intron of an annotated gene named *tmem180* (Fig. 5a). However, the cytokines, including IL-4, IL-10, or IL-13 had no effect on the expression of *tmem180* gene (Fig. 4c), implying that miR-146b could be transcribed independent of *tmem180* transcript in macrophages. Then, we looked at the putative promoter regions covering 2000 bp upstream of the coding region of *pre-miR-146b*, and identified one conserved putative binding site for STAT3, one site for STAT6, and one site for both STAT3 and STAT6 (Fig. 5a). The STAT3 and STAT6 are the main transcription factors mediating IL-10 and IL-4/13 signalling, respectively, and it has been shown that miR-146b is a direct target gene of STAT3 (Curtale et al., 2013; Xiang et

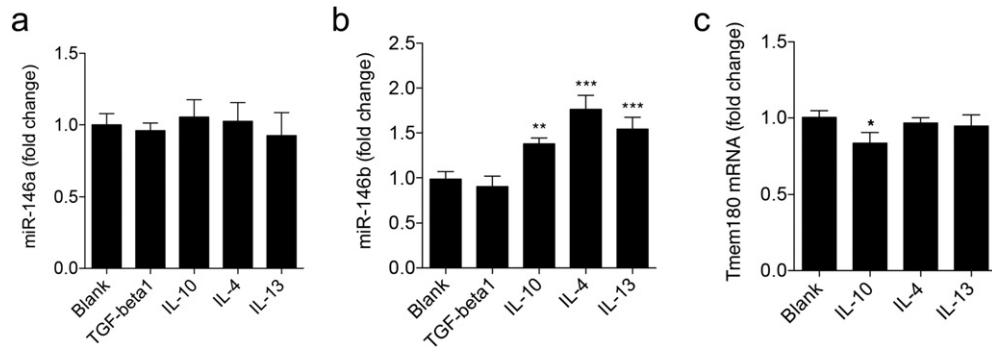


**Fig. 4.** IL-4/10/13 induced miR-146 expression in BMDMs. Expression levels of miR-146a (a), miR-146b (b) and Tmem180 (c) in BMDMs after stimulation with TGF- $\beta$ 1, IL-4, IL-10, or IL-13 for 12 h. \* $P < 0.05$ , \*\* $P < 0.01$ , \*\*\* $P < 0.001$ , compared with blank control samples. Data are shown as means with SDs. Data in all panels are representative of four independent experiments.

al., 2014). To investigate the role of these putative binding sites in regulating the Th2 cytokine-dependent transcription, we generated a construct expressing luciferase under the control of the putative promoter (Fig. 5a). We showed that all the Th2 cytokines including IL-4, IL-10, and IL-13 significantly upregulated the expression of the luciferase reporter gene in BMDMs (Fig. 5b), which indicated that the STAT3- and STAT6- binding sites in the promoter mediate the cytokine-dependent transcription. In addition, we used ChIP analysis to further validate the activity of these putative binding sites. In the ChIP analysis, we designed two pairs of primers to detect the binding of STAT3/6 to these putative sites, one of which (primer 1) covered the STAT6 site, and the other (primer 2) covered the STAT3 site and common site for STAT3/6 (Fig. 5a). Our results showed that, in IL-10 stimulated macrophages, STAT3 was recruited to the *pre-miR-146b* promoter, as the enrichment of putative STAT3 site detected by primer 2 was significantly elevated after stimulation. STAT6-dependant recruitment to the *pre-miR-146b* promoter was also observed in the IL-4/13 stimulated macrophages, but STAT6 seemed to bind to different regions in different situations. In IL-4 stimulated macrophages, STAT6 was recruited to the region

detected by primer 2, while in IL-13 stimulated macrophages, STAT6 was recruited to the region detected by primer 1 (Fig. 5c).

### 3.5. Th2 cytokines inhibit the differentiation of macrophages to M1 cells by induction of miR-146b

Th2 cytokines can block IFN- $\gamma$ -induced activation of macrophages, but the mechanism is not yet clear (Sica and Mantovani, 2012). As shown in Fig. 6a, all the Th2 cytokines including IL-4, IL-10 and IL-13 potentially inhibited IFN- $\gamma$ -induced iNOS production in the Kupffer cell line. We postulated that these cytokines induced the elevation of miR-146b, which in turn blocked the activation of the macrophages. To test this, we first transfected Kupffer cells with either transfection reagent (mock group) or negative control inhibitors (NC group) or miR-146b inhibitors (anti-miR-146b group), and then stimulated them with IL-4 or IL-10 or IL-13, followed by IFN- $\gamma$  stimulation. Our data showed that compared with mock and NC group, the expression of iNOS in the anti-miR-146b group was significantly elevated, indicating that downregulation of

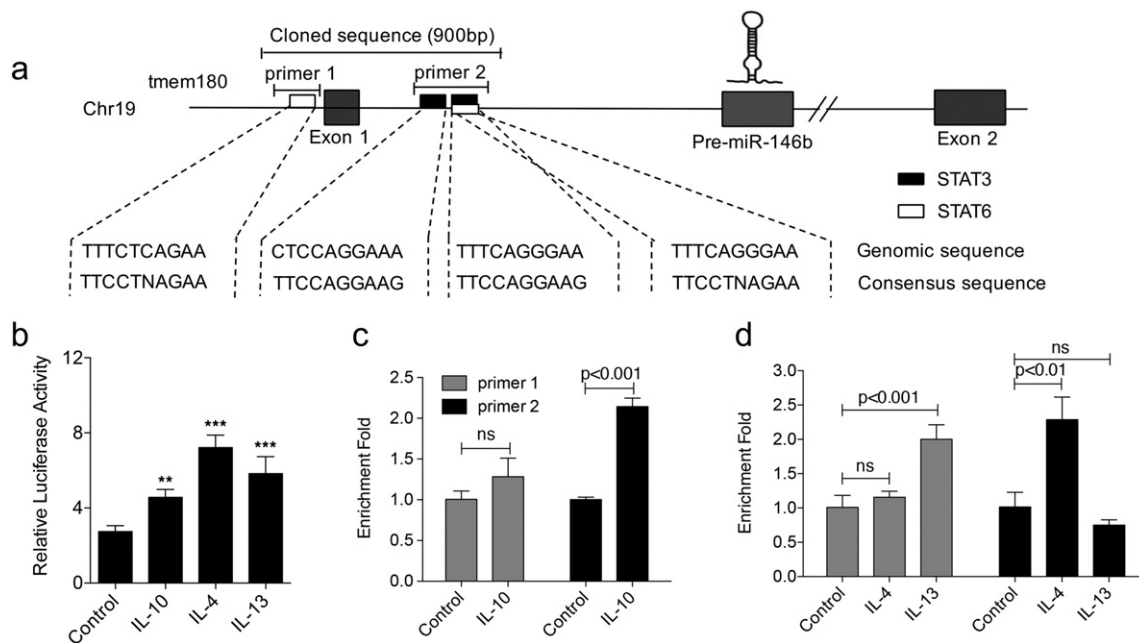


**Fig. 5.** IL-4/10/13 induced miR-146 expression in BMDMs by activating the promoter of the *pre-miR-146* gene. (a) Schematic diagram of the *miR-146b* genomic locus on murine chromosome 19. Predicted binding sites of STAT3 (black) and STAT6 (white) transcription factors are shown as boxes. (b) The genomic region indicated by the bar above the miR-146b locus was analysed in a promoter luciferase reporter assay. \* $P < 0.05$ , \*\* $P < 0.01$ , \*\*\* $P < 0.001$ , compared with control samples. (c) BMDMs were stimulated for 12 h with IL-4, IL-10 or IL-13, or not stimulated (control), and ChIP assays were carried out by using anti-STAT3 or anti-STAT6 antibody and analysed by qPCR with specific primers binding to the *miR-146b* promoter. Data are shown as means with SDs. Data in all panels are representative of three independent experiments.

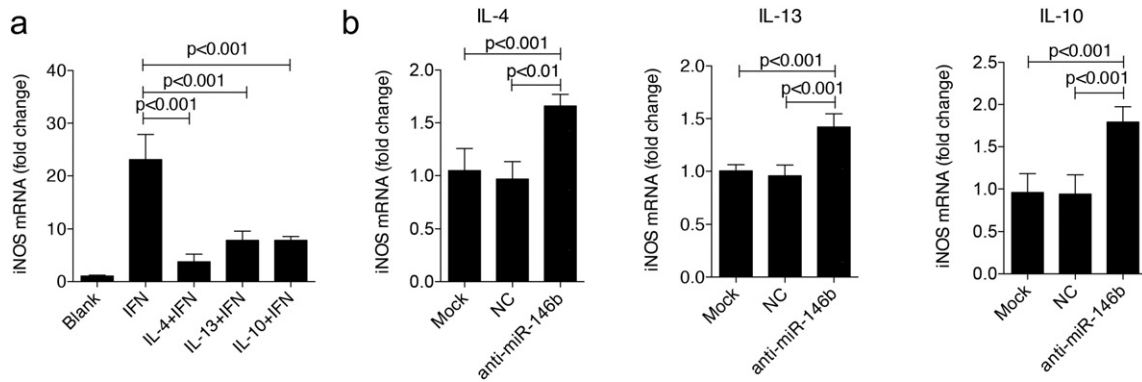


**Fig. 6.** Inhibition of miR-146b blocked the effect of IL-4/10/13 on the IFN- $\gamma$ -induced activation of macrophages. (a) iNOS production in a Kupffer cell line pretreated with IL-4, IL-10 or IL-13 for 12 h, followed by the addition of IFN- $\gamma$ . (b) A Kupffer cell line was transfected with 40 nM miR-146b inhibitor, negative control inhibitor (NC), or transfection reagent only (mock) for 12 h, then pretreated with IL-4 or IL-10 or IL-13 for 12 h, followed by the addition of IFN- $\gamma$ . Total RNA was extracted and analysed for iNOS expression by qPCR. Data are shown as means with SDs. Data in all panels are representative of four independent experiments.

miR-146b expression relieved the inhibitory effect of the Th2 cytokines on the IFN- $\gamma$ -induced activation of M1 macrophages (Fig. 6b).

#### 4. Discussion

Macrophages have been reported to modulate the initiation, maintenance, and resolution of schistosomiasis through differentiating to various activation states, and therefore, a therapy designed to manipulate macrophage activation could be a relevant approach to treat this chronic disease. However, to date, no well-validated targets have been identified in macrophages in order to treat this disease. In this study, we found that miR-146a/b were primarily expressed in the hepatic macrophages, and that miR-146a/b inhibited the differentiation of macrophages to M1 cells by targeting STAT1. Importantly, we found that various Th2 cytokines, including IL-4, IL-10, and IL-13, could induce macrophages to express miR-146b, but not miR-146a, by activating the promoter of *pre-miR-146b* gene. Further, these cytokines could potentially block the differentiation of macrophages to M1 macrophages, partly by induction of miR-146b. Thus, our data indicated that miR-146 played an important role in the regulation of macrophage activation during hepatic schistosomiasis.

Schistosomes are a prime example of a complex multicellular pathogen that survives in the host despite the development of a significant immune response, and understanding how the immune system acts against this parasite is still a daunting challenge. It is well documented that macrophages, key cells of the immune system, play a central role in the immunopathology induced by schistosome eggs by differentiating into various phenotypes. Several studies have highlighted that prompt transition of macrophages from M1 cells to M2 cells is critical for the host to survive in cases of acute schistosomiasis (Herbert et al., 2004), however, little is known about the mechanisms that regulate the transition between macrophage phenotypes. Here, our study implies that miR-146 might be an important mediator in this process, and our data suggest that at the early stage of infection including the migration of the schistosomula and adult worms, the dominant immune response is Th1 type and elevated IFN- $\gamma$  levels stimulate macrophages to differentiate to M1 cells through activation of STAT1. When the parasites begin to produce eggs, the host immunity switches to a Th2 response and upregulated Th2 cytokines begin to induce the macrophages to differentiate to M2 cells, and meanwhile, these cytokines such as IL-10 and IL-4/13 also induce the expression of miR-146b by activating STAT3/6, which bind to the promoter of the *pre-miR-146b* gene and initiate transcription. The resulting miR-146b further inhibits the differentiation of M1 macrophages by targeting STAT1 (Fig. 7). Considering the fact that prompt transition of macrophages from M1 cells to M2 cells is critical for host to survive in the

acute schistosomiasis, we speculated that miR-146 could be a crucial protective factor for host in the acute stage of infection, and played an important role in the transition from acute to chronic infection. It is worthy to point out that, though we did not explore it in this study, miR-146 might also be involved in the regulation of other immune cells, such as B cells and T cells, which are essential for the development of hepatic schistosomiasis (Pearce and MacDonald, 2002).

Schistosomiasis is a debilitating and chronic disease associated with egg-induced inflammation, tissue damage, and subsequent fibrosis. The highly desirable outcome in the treatment of schistosomiasis is to resolve inflammation, reverse fibrosis, and restore normal tissue architecture and function (Barron and Wynn, 2011). Numerous studies have established that M1 macrophages are related to inflammation and tissue damage, but are capable of remodelling the ECMs, while M2 macrophages are essential for hosts to survive the acute phase of infection, but are involved in fibrosis (Barron and Wynn, 2011). Thus, therapies designed to manipulate macrophage activation appear suitable for treating this chronic disease. It is reasonable that development of slightly more M1 than M2 macrophages will be beneficial to provide the greatest degree of protection during infection by minimizing fibrosis, while simultaneously protecting the host from tissue damage. In this study, we have investigated whether miR-146 could manipulate macrophage activation and have a potential for treating schistosomiasis through regulating differentiation of macrophages. *S. japonicum* infection can elevate the expression of miR-146 that could block differentiation of hepatic macrophages into M1 cells by targeting STAT1. Thus, manipulation of the expression of miR-146 could result in more macrophages differentiating into M1-type, leading to elevated iNOS expression that might attenuate the formation of egg granuloma and fibrosis (Wynn et al., 1995). In addition, the degree of target inhibition imposed by miRNAs always tends to be modest (Ebert and Sharp, 2012), thus, through intervening miRNA expression, the pathway regulated by miRNA in macrophages seemed not to be totally blocked or activated, which is essential for hosts to survive in the course of infection. Therefore, miR-146 appears to be an ideal target for manipulating macrophage activation. However, we have to admit that the hepatic macrophages, defined as CD11b positive cells in this study, might be a mixed population (a proliferating resident macrophages and monocyte-derived macrophages), especially at latter infection time, as a recent study has shown that macrophages in the hepatic granulomas were predominantly derived from monocytes during *S. mansoni* infection (Nascimento et al., 2014).

miR-146a and miR-146b are two miRNAs of the same family that share the same seed sequence and only differ by two nucleotides at the 3' end in their mature sequences. However, they are encoded by distinct genes located on separate chromosomes, which implies that they

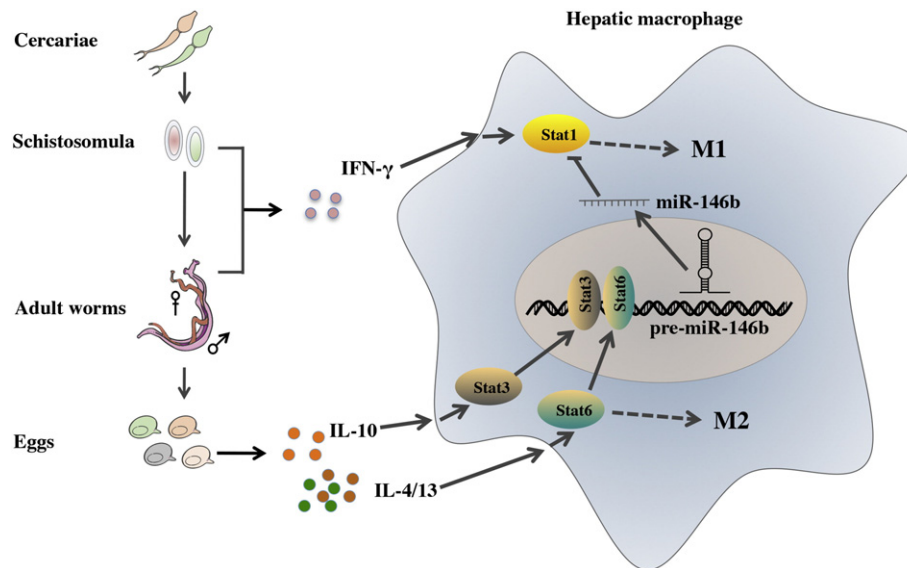


**Fig. 7.** Schematic diagram of the role of miR-146b in the regulation of activation of macrophages during hepatic schistosomiasis. At the early stage of infection, the schistosomula and adult worms induced Th1 immune response and elevated IFN- $\gamma$  level that stimulates the differentiation of macrophages to M1 cells through activation of STAT1. When the parasites begin to produce eggs, the host immune response switches from a Th1 to a Th2 type and upregulated Th2 cytokines such as IL-4/13 that stimulate differentiation of macrophages to M2 cells through activation of STAT6. Meanwhile, the Th2 cytokines of IL-10 and IL-4/13 induce the expression of miR-146b by activating STAT3 and STAT6, respectively, which bind to the promoter of the *pre-miR-146b* gene and initiate transcription. The resulting miR-146b inhibits the differentiation of M1 macrophages by targeting STAT1.

may fulfil distinct functions. Indeed, experimental evidences have demonstrated that both miR-146a and miR-146b are involved in the regulation of macrophage activation, but their target genes and biological roles are different (Nahid et al., 2011; Saba et al., 2014). The gene encoding miR-146a in macrophages was rapidly induced by pro-inflammatory factors, such as LPS and IL-1 $\beta$ , which activate the nuclear factor kappa B (NF- $\kappa$ B) pathway, but the elevated miR-146a blocks further activation of NF- $\kappa$ B signaling, forming a negative feedback loop (Perry et al., 2008; Taganov et al., 2006). While miR-146b expression is also enforced in the macrophages by LPS stimulation with delayed kinetics with respect to miR-146a and via an IL-10-mediated STAT3-dependent transcription, indicating that miR-146b is involved in the IL-10-dependent resolution phase of inflammation (Curtale et al., 2013). In addition, several studies have revealed that miR-146a directly inhibits the activation of M1 macrophage and plays an important role in the pathogenesis of human diseases, such as *Brugia malayi* infection (Rückerl et al., 2012), mycobacterial exposure (Li et al., 2016), and nephropathy (Bhatt et al., 2016). By contrast, miR-146b has not been reported to have such a function. In this study, we found that, although both miR-146a and miR-146b were up-regulated in the process of schistosome infection, only miR-146b could be induced by a series of Th2 cytokines involved in the chronic stage of infection, by activating STAT3/6, and the Th2 cytokines, at least partly, inhibited the differentiation of macrophages to M1 cells by induction of miR-146b through targeting STAT1. Thus, our study further demonstrated the distinct regulations and biological roles of miR-146a and miR-146b in macrophages. Importantly, data from this study reveal an inhibitory effect of Th2 cytokines such as IL-10 and IL-4/13 on the activation of M1 macrophages through induction of miR-146b.

In summary, considering the role of macrophages in the hepatic immunopathology induced by schistosome eggs, there is a need to explore therapeutic strategies designed to manipulate macrophage activation to treat this chronic disease. Our data indicate the protective roles of miR-146a/b in hepatic schistosomiasis through regulating differentiation of macrophages into M2 cells.

#### Funding Sources

This work was supported by grants from the National Natural Science Foundation of China (81430051 and 81501767).

#### Conflict of Interest

We declare no financial or other relationship causing conflict of interest in this study.

#### Author Contributions

X.H., D.M.Z., K.Y.Z. and W.Q.P. designed the project, X.H., R.T., and W.Q.P. analysed the results and wrote the manuscript. X.H., R.T., Y.S. and Y.G.W. performed the experimental work.

#### Acknowledgments

We thank the staff of the National Institute of Parasitic Disease, Chinese Center for Disease Control and Prevention for their help with parasite infections.

#### Appendix A. Supplementary data

Supplementary data to this article can be found online at <http://dx.doi.org/10.1016/j.ebiom.2016.10.024>.

#### References

- Barron, L., Wynn, T.A., 2011. Macrophage activation governs schistosomiasis-induced inflammation and fibrosis. *Eur. J. Immunol.* 41, 2509–2514.
- Bartel, D.P., 2004. MicroRNAs: genomics, biogenesis, mechanism, and function. *Cell* 116, 281–297.
- Bartel, D.P., 2009. MicroRNAs: target recognition and regulatory functions. *Cell* 136, 215–233.
- Bhatt, K., Lanting, L.L., Jia, Y., et al., 2016. Anti-inflammatory role of microRNA-146a in the pathogenesis of diabetic nephropathy. *J. Am. Soc. Nephrol.* 27, 2277–2288.
- Burke, M.L., Jones, M.K., Gobert, G.N., et al., 2009. Immunopathogenesis of human schistosomiasis. *Parasite Immunol.* 31, 163–176.
- Cai, P., Piao, X., Liu, S., et al., 2013. MicroRNA-gene expression network in murine liver during *Schistosoma japonicum* infection. *PLoS One* 8, e67037.
- Cai, P., Gobert, G.N., McManus, D.P., 2016. MicroRNAs in parasitic helminthiasis: current status and future perspectives. *Trends Parasitol.* 32, 71–86.
- Colley, D.G., Bustinduy, A.L., Secor, W.E., et al., 2014. Human schistosomiasis. *Lancet* 383, 2253–2264.
- Curtale, G., Mirolo, M., Renzi, T.A., et al., 2013. Negative regulation of Toll-like receptor 4 signaling by IL-10-dependent microRNA-146b. *Proc. Natl. Acad. Sci. U. S. A.* 110, 11499–11504.

- Davis, B.K., 2013. Isolation, culture, and functional evaluation of bone marrow-derived macrophages. *Methods Mol. Biol.* 1031, 27–35.
- Ebert, M.S., Sharp, P.A., 2012. Roles for microRNAs in conferring robustness to biological processes. *Cell* 149, 515–524.
- Han, H., Peng, J., Hong, Y., et al., 2013. MicroRNA expression profile in different tissues of BALB/c mice in the early phase of *Schistosoma japonicum* infection. *Mol. Biochem. Parasitol.* 188, 1–9.
- He, X., Sai, X., Chen, C., et al., 2013. Host serum miR-223 is a potential new biomarker for *Schistosoma japonicum* infection and the response to chemotherapy. *Parasit. Vectors* 6, 272.
- He, X., Pu, G., Tang, R., et al., 2014. Activation of nuclear factor kappa B in the hepatic stellate cells of mice with schistosomiasis japonica. *PLoS One* 9, e104323.
- He, X., Xie, J., Zhang, D., et al., 2015. Recombinant adeno-associated virus-mediated inhibition of microRNA-21 protects mice against the lethal schistosome infection by repressing both IL-13 and transforming growth factor beta 1 pathways. *Hepatology* 61, 2008–2017.
- Herbert, D.R., Hölscher, C., Mohrs, M., et al., 2004. Alternative macrophage activation is essential for survival during schistosomiasis and downmodulates T helper 1 responses and immunopathology. *Immunity* 20, 623–635.
- Kreider, T., Anthony, R.M., Urban Jr., J.F., et al., 2007. Alternatively activated macrophages in helminth infections. *Curr. Opin. Immunol.* 19, 448–453.
- Lee, T.L., Johnstone, S.E., Young, R.A., 2006. Chromatin immunoprecipitation and microarray-based analysis of protein location. *Nat. Protoc.* 1, 729–748.
- Li, M., Wang, J., Fang, Y., et al., 2016. microRNA-146a promotes mycobacterial survival in macrophages through suppressing nitric oxide production. *Sci. Rep.* 6, 23351.
- Lu, L.F., Boldin, M.P., Chaudhry, A., et al., 2010. Function of miR-146a in controlling Treg cell-mediated regulation of Th1 responses. *Cell* 142, 914–929.
- Ma, X., Buscaglia, L.E.B., Barker, J.R., et al., 2011. MicroRNAs in NF- $\kappa$ B signaling. *J. Mol. Cell Biol.* 3, 159–166.
- Nahid, M.A., Satoh, M., Chan, E.K., 2011. Mechanistic role of microRNA-146a in endotoxin-induced differential cross-regulation of TLR signaling. *J. Immunol.* 186, 1723–1734.
- Nascimento, M., Huang, S.C., Smith, A., et al., 2014. Ly6Chi monocyte recruitment is responsible for Th2 associated host-protective macrophage accumulation in liver inflammation due to schistosomiasis. *PLoS Pathog.* 10, e1004282.
- Noël, W., Raes, G., Hassanzadeh Ghassabeh, G., et al., 2004. Alternatively activated macrophages during parasite infections. *Trends Parasitol.* 20, 126–133.
- Pearce, E.J., MacDonald, A.S., 2002. The immunobiology of schistosomiasis. *Nat. Rev. Immunol.* 2, 499–511.
- Perry, M.M., Moschos, S.A., Williams, A.E., et al., 2008. Rapid changes in microRNA-146a expression negatively regulate the IL-1beta-induced inflammatory response in human lung alveolar epithelial cells. *J. Immunol.* 180, 5689–5698.
- Rückerl, D., Jenkins, S.J., Laqtom, N.N., et al., 2012. Induction of IL-4R $\alpha$ -dependent microRNAs identifies PI3K/Akt signaling as essential for IL-4-driven murine macrophage proliferation in vivo. *Blood* 120 (2307–2016).
- Saba, R., Sorensen, D.L., Booth, S.A., 2014. MicroRNA-146a: a dominant, negative regulator of the innate immune response. *Front. Immunol.* 5, 578.
- Schmittgen, T.D., Livak, K.J., 2008. Analyzing real-time PCR data by the comparative C(T) method. *Nat. Protoc.* 3, 1101–1108.
- Shainheit, M.G., Smith, P.M., Bazzone, L.E., et al., 2008. Dendritic cell IL-23 and IL-1 production in response to schistosome eggs induces Th17 cells in a mouse strain prone to severe immunopathology. *J. Immunol.* 181, 8559–8567.
- Sica, A., Mantovani, A., 2012. Macrophage plasticity and polarization: in vivo veritas. *J. Clin. Invest.* 122, 787–795.
- Taganov, K.D., Boldin, M.P., Chang, K.J., et al., 2006. NF-kappaB-dependent induction of microRNA miR-146, an inhibitor targeted to signaling proteins of innate immune responses. *Proc. Natl. Acad. Sci. U. S. A.* 103, 12481–12486.
- Tang, Y., Luo, X., Cui, H., et al., 2009. MicroRNA-146a contributes to abnormal activation of the type I interferon pathway in human lupus by targeting the key signaling proteins. *Arthritis Rheum.* 60, 1065–1075.
- Wynn, T.A., Cheever, A.W., Jankovic, D., et al., 1995. An IL-12-based vaccination method for preventing fibrosis induced by schistosome infection. *Nature* 376, 594–596.
- Xiang, M., Birkbak, N.J., Vafaizadeh, V., et al., 2014. STAT3 induction of miR-146b forms a feedback loop to inhibit the NF- $\kappa$ B to IL-6 signaling axis and STAT3-driven cancer phenotypes. *Sci. Signal.* 7, ra11.